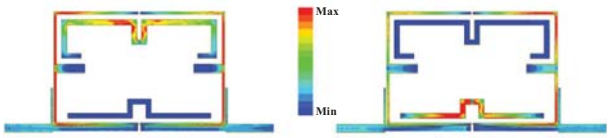

Fig. 3 Simulated current distributions of the proposed DBBPF: (a) at 2 GHz, (b) at 3.5 GHz

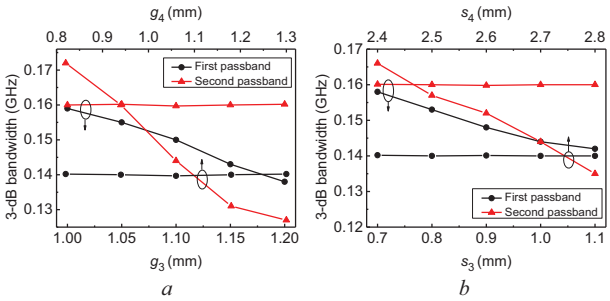

Fig. 4 Simulated bandwidths against filter dimensions. (a) Simulated bandwidths against different g_3 and g_4 when $s_3 = 0.81$ mm and $s_4 = 2.58$ mm. (b) Simulated bandwidths against different S_3 and S_4 when $g_3 = 1.11$ mm, $g_4 = 0.95$ mm

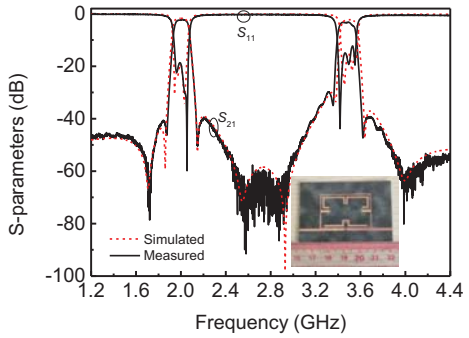

Fig. 5 Measured results of the proposed DBBPF in comparison with the simulations

Measured results: The DBBPF was fabricated on a Rogers 5880 substrate board with a thickness of 0.508 mm and relative permittivity of 2.2. The inset in Figure 5 is a photograph of the fabricated filter. The measurements were carried out by Agilent E8363B network analyser. The measured results are given in Figure 5, showing a good agreement with the simulations. The measured dual-band centre frequencies are located at 2 and 3.48 GHz with 3-dB fractional bandwidths of 6.5% and 4.3%, respectively. The measured in-band insertion losses (ILs) and return losses for the first/second passband are 2.28/3.33 dB and 18/12 dB, respectively. Four pairs of TZs are clearly identifiable in the stopband, resulting in very high frequency selectivity and high isolation between the passbands. The filter has a compact size of $0.19\lambda_g \times 0.32\lambda_g$, where λ_g is the guided wavelength at 2 GHz. Table 1 compares the performances between this filter and several prior works. The presented work exhibits very competitive performance, particularly in comparison with the fully-canonical DBBPF in [6]. The proposed DBBPF features independent controllable bandwidths and more compact size.

Conclusion: A microstrip fourth-order fully-canonical DBBPF has been designed and verified experimentally in this letter. The proposed filter exhibits the merits of compactness, high frequency selectivity, high isolation between passbands, and independently controllable bandwidths. It demonstrates a novel and effective circuit technique for high-performance dual-band filters.

Table 1. Comparison with several prior DBBPFs

Ref.	f_{01}/f_{02}(GHz)	IL(dB)	O	TZs	CB	F	Size ($\lambda_g \times \lambda_g$)
[1]	2.36/5.83	1.1/1.6	2/2	5	Y	N	0.16 × 0.18
[2]	2.4/5.2	1.4/1.76	4/4	4	Y	N	0.21 × 0.35
[3]	1.84/2.65	0.43/0.65	2/2	4	N	N	0.17 × 0.21
[4]	1.8/3.5	0.8/0.9	2/2	5	Y	N	0.15 × 0.12
[5]	1.98/3.52	0.82/0.84	3/3	7	N	N	N/A
[6]	1.8/5.8	1.21/3.89	4/4	8	N	Y	0.247 × 0.494
This work	2/3.48	2.28/3.33	4/4	8	Y	Y	0.19 × 0.32

O: orders; CB: controllable bandwidth; F: Fully-canonical response; N: No; Y: Yes; N/A: non-available.

Received: *27 July 2020* Accepted: *5 October 2020*
doi: 10.1049/ell2.12027

References

1 Ren, B.P. et al.: Miniature dual-band bandpass filter using modified quarter-wavelength SIRs with controllable passbands. *Electron. Lett.* **55**(1), 38–40 (2019)
2 Yan, J.M. et al.: Design of a fourth-order dual-band bandpass filter with independently controlled external and inter-resonator coupling. *IEEE Microw. Wireless Compon. Lett.* **25**(10), 642–644 (2015)
3 Yang, S. et al.: Design of compact dual-band bandpass filter using dual-mode stepped-impedance stub resonators. *IEEE Microw. Wireless Compon. Lett.* **26**(9), 672–674 (2016)
4 Gao, L., Zhang, X.Y.: High-selectivity dual-band filter using a quad-mode resonator with source-load coupling. *IEEE Microw. Wireless Compon. Lett.* **23**(9), 474–476 (2013)
5 Tang, M.C et al.: Dual-band bandpass filter based on a single triple-mode ring resonator. *Electron. Lett.* **52**(9), 722–724 (2016)
6 Zhang, S.B, Zhu, L.: Fully canonical dual-band bandpass filter with λ/4 stepped impedance resonators. *Electron. Lett.* **50**(3), 192–194 (2014)
7 Cameron, R.J.: Advanced coupling matrix synthesis techniques for microwave filters. *IEEE Trans. Microw. Theory Tech.* **51**(1), 1–10 (2003)
8 Hong, J.S.: *Microstrip Filters for RF/Microwave Applications*. 2nd ed., Wiley, Hoboken, NJ (2011)

Multi-resonator application on size reduction for retransmission-based chipless RFID tag

A. K. M. Z. Hossain,[1] M. I. Ibrahimy,[2,✉] S. M. A. Motakabber,[2] S. M. K. Azam,[2] and M. S. Islam[2]
[1] *Centre for Telecommunication Research & Innovation (CeTRI), Fakulti Teknologi Kejuruteraan Elektrik & Elektronik (FTKEE), Universiti Teknikal Malaysia Melaka (UTeM), Malacca, Malaysia*
[2] *Department of Electrical and Computer Engineering (ECE), Faculty of Engineering (KoE), International Islamic University Malaysia (IIUM), Kuala Lumpur, Malaysia*
✉ Email: ibrahimy@iium.edu.my

Here, a 'truncated C'-shaped planar coupled line resonator for UWB retransmission-based chipless RFID has been presented. The resonator

is small compared to other existing resonators in the retransmission-based chipless RFID family. Two different coded multi-resonator prototype tags have been designed and validated with newly designed planar microstrip fingertip-shaped antennas. A good agreement is found between simulation and measurement responses. From the system validation, different coding combinations have been extracted when all resonators are present (111111111) and when three resonators are absent (110110101). It is found that with this resonator, 9 bits can be imposed instead of the existing planar rectangular resonator that gives only 1 bit with a larger size. Hence, as much as 86.7% of the occupied area is reduced by the resonator presented in this work. This work is anticipated to motivate the researchers in developing UWB passive RFID tags with higher bit density and smaller sizes for item tagging and sensing applications.

Introduction: Radio frequency identification (RFID), a term that nowadays is getting very popular both for researchers and consumers. Every day, from toll collection to inventory management, and from item tagging to sensing, RFID is taking its parts either in the consumer level or in the research and development. Most of commercially deployed RFID systems are passive by nature and come up with chip. Despite chipped tags have the advantage of high EPC global bits (96–124) for encryption, the presence of chip makes them expensive [1]. The solution of this issue is to make the RFID tags chipless. However, that comes up with a cost of low bits for encryption. Most of the chipless tags are designed for UWB region by following the on-off keying (OOK) technique for data bit coding where the number of resonators' presence/absence (logic state 1/0 or 0/1) determines the number of actual bits for coding. As a result, such a dependency restricts the researchers to include a large number of bits since this has effects on increasing the size of the tag proportionally which in turn produces a low bit density (i.e. bits/area, bits/GHz etc.) of chipless tags compared to the existing commercial passive IC tags.

The chipless tags may be employed with (retransmission-based) or without (backscatter and RCS-based) antenna(s) on board. The RCS-based tags are smaller in size, but the detection process depends on three separate measurements (without tag, with tag, and a reference tag) to calculate the RCS for frequency domain coding which is troublesome and tedious. Furthermore, the reader's Tx and Rx antennas (sometimes a single Tx/Rx antenna) have same polarization that leads to include cross talks. Hence, it becomes troublesome for tag detection [2]. On the other hand, due to the antenna on board, the retransmission-based tags are larger compared to the RCS-based tags. However, the retransmission-based detection process is very straightforward. Only a single S-parameter (magnitude and/or phase) measurement in frequency domain with the presence of the tag is needed for extracting the bits. In addition, the separate Tx and Rx reader and tag antennas have 90^0 polarization mismatch which makes the system theoretically isolated and interference-free between the sending and receiving signals. Keeping these advantages in mind, the focus is now to make the retransmission based tags with high bit density. As the dimensions of the antennas cannot be changed, this can be done basically in two different ways-either (solution-1) resonators are needed to be designed in a way that each resonator can be used for multiple states of bit combinations, or (solution-2) the resonator itself is designed with smaller size that replaces the existing resonators with multiple bits instead, to produce high bit density re-transmission based tags. Usually, a coding follows the binary system in chipless tags, and if the number of resonators on board is N, the number of coding combinations are 2^N. Now, if the number of coding states are M ($2 < M$), then M^N combinations can be generated with the solution-1. By keeping the same numbers of bits on board, bit combinations can be increased. On the other hand, the solution-2 deals with the direct approach on the miniaturization of the resonator elements to accommodate a higher N numbers in the same occupied area to produce high bit density tags.

One of the early researches has been done by [1] where a retransmission type 35-bit tag for the Australian banknote detection is introduced but in cost of a large area of 85×55 mm^2 by using magnitude and phase responses of the S-parameter (S_{21}). The microstrip rectangular spiral resonators (MRSR) are used as the resonating bit element there. The dimension of the resonator is 5.2×6 mm^2 (width $\times$ length) at 3.5 GHz resonance. Lengths and turns of the resonators are changed to produce different resonator structures that represent different resonant

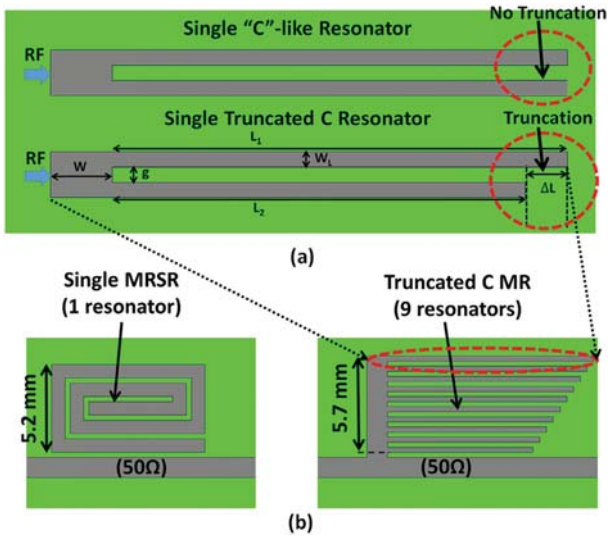

Fig. 1 *TCR construction and comparisons (a) Single TCR & 'C'-like resonator ($W = 1.2$ mm, $L_1 = 10.3$ mm, $L_2 = 10.1$ mm, $W_L = g = 0.3$ mm and $\Delta L = 0.2$ mm) (b) comparison of TCMR with the existing MRSR*

frequencies while keeping the width unchanged as it has no effect on the resonance. By employing 35 different resonators, a 35-bit tag has been achieved. Following the solution-1 stated earlier, in [3], same MRSR is used to design a chipless tag by utilizing only the phase response, where, it has been shown that one single resonator structure can encode three different coding states. By employing the coupled lines at the output and the input ports, and with the change of the resonator positions on the coupled lines, different states are created for bit coding. Recently in [4] and [5], the coupled line rectangular resonator structure is adopted to design a 3-state and a k-state resonator, respectively. For the 3-state resonator, a 4×8.5 mm^2 rectangular structure with three horizontal parallel coupled line arms are used. By connecting and disconnecting particular arm(s) with the rectangular frame of the resonator, the different bit states are achieved. In the similar way, the K-state resonator is built also which have a dimension of 5.5×9.4 mm^2. However, the parallel coupled line arms are positioned as vertical instead of horizontal in [4]. To encode different bit state, a particular arm is connected with the main rectangle structure, and the rest are kept disconnected. Nevertheless, no focus is given on decreasing the dimensions of the resonators. In [6], an approach has been done to reduce the dimension of the resonator (solution-2) by proposing a microstrip circular spiral resonator (MCSR) as the resonating element. Even though the MCSR reduced around 9.8% of the area taken by the MRSR but due to the low Q-factor (quality-factor), the resonator is difficult to be implemented for high number of bits. In [2], the modified complementary split ring resonator (MCSRR), and in [7], the complementary split ring resonator (CSRR) have been proposed as the resonating elements and implemented on chipless tags. However, both resonators are yet large and incompatible for high bit chipless tags, and thus ended up with 8-bit and 6-bit tag respectively.

To address the major issues mentioned so far, in this letter, with the 'truncated C' resonator (TCR), 9-bit multi-resonators (MR) have been designed and implemented for the system validation through retransmission. A remarkable area has been reduced by the implemented MR compared to the conventional resonators used for the same application. Furthermore, the application has been shown to validate MR's suitability for the fully chipless RFID system.

Multi-Resonator Design: For the RCS-based chipless tags, the 'C'-like resonators as in [8] are employed. Here, from the initiation in [9], a planar coupled line 'truncated C'-shaped resonator has been utilized in this work for the retransmission-based chipless tags. Figure 1a illustrates the comparison of the structural differences between TCR (with detailed dimensions) and 'C'-like resonator. The comparison between the existing MRSR and the truncated C multi-resonator (TCMR) is given in Figure 1b. The proposed resonator structure is named as 'truncated C' because the two parallel arms of the "C" are not equal ($L_1 \neq L_2$), and the

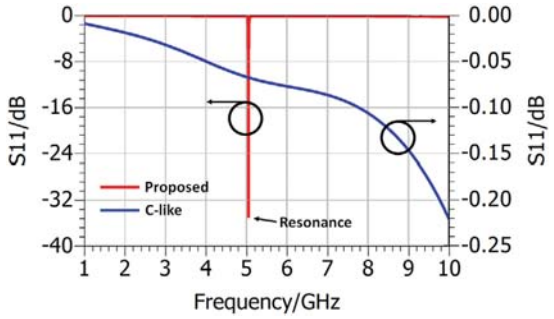

Fig. 2 *Analysed S-parameter of TCR and C-like resonator*

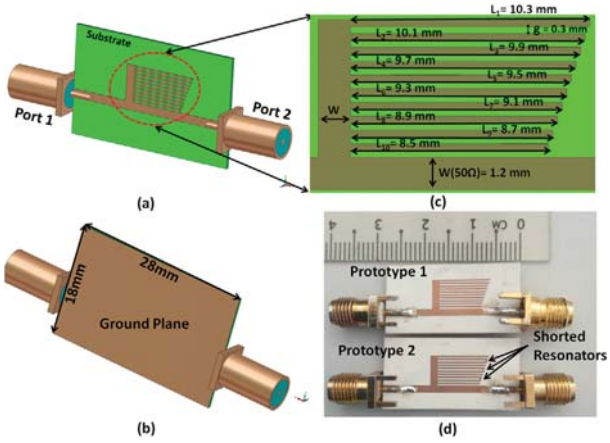

Fig. 3 *Development of TCMR prototypes (a) 9-bit TCMR front view (b) 9-bit TCMR back view (c) TCMR's exploded view with dimensions (d) two differently coded pretotypes*

lower arm is truncated with a factor of $\Delta L = L_1 - L_2$; this is the basic difference of TCR from the C-like resonator as seen from Figure 1(a). In fact, the ΔL imposes a key effect on implementing the resonator in a retransmission-based chipless tag. From their S-parameter analyses, Figure 2 illustrates the difference of responses between these two resonators. It is seen that the 'C'-like (no truncation, $\Delta L = 0$) resonator does not resonate at all within the desired frequency range. Whereas, the proposed TCR ($\Delta L \neq 0$) gives a significantly noticeable resonance by giving a sharp dip as low as -35 dB while being excited directly through the RF feed. Thus, the TCR obtains the suitability for retransmission-based chipless RFIDs. The ΔL value is chosen as 0.2 mm that gives a sharp enough dip at the resonance point. Referred back to Figure 1b, the TCMR structure is constructed by nine different TCRs. It can be seen that two parallel arms and one gap are needed to make a single bit resonator. Consequently, the occupied area of the TCR becomes 10.35 mm^2 as the length (L_1) and width ($2W_L + g$) are 11.5 and 0.9 mm, respectively. Likewise, three arms and two gaps are required to construct a two bit MR structure. In this way, if the width (5.2 mm) of the existing MRSR is utilized, 8.1 resonators can be accommodated. Since the physical resonator cannot be fractioned, one more resonator (one arm and a gap) has been added to build the 9-resonator (9-bit) TCMR structure that has the width of 5.7 mm ($10W_L + 9g$) and a maximum length of 11.5 mm.

By utilizing the width of MRSR (one bit) structure, several bits can be accommodated. The layout of TCMR has been implemented with 50 Ω transmission line (TL) as illustrated in Figure 3 which makes it a 9-bit structure for the chipless tag (without antennas). Figure 3c demonstrates the exploded view of the TCMR section with TL with the necessary dimensions. The substrate material used in this design is Rogers 3003 (relative dielectric permittivity, $\varepsilon_r = 3$; substrate height, $h = 0.51$ mm; and loss tangent, tan $\delta = 0.001$). Advanced Design System 2019 has been used for the electromagnetic simulation. Prototypes of two differently coded 9-bit MR have been developed as presented in Figure 3d. All of nine resonators are present (logic '1′ for presence and logic '0′ for absence) in the prototype 1 which makes the coding combination as '111111111′. In the prototype 2, three different (3rd, 6th, and 8th) resonators are shorted which makes the coding combination as '110110101′.

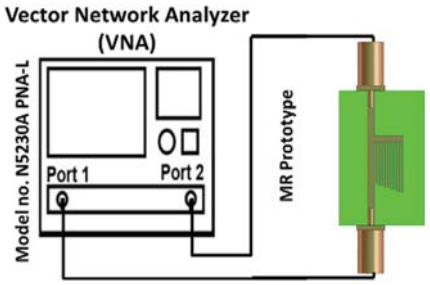

Fig. 4 *Experimental setup for TCMR Validation*

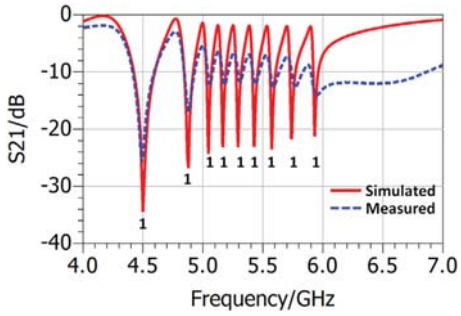

Fig. 5 *S_{21} response for prototype 1*

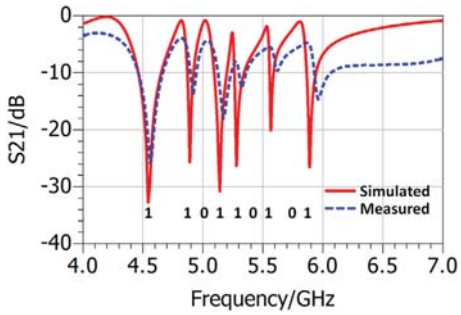

Fig. 6 *S_{21} response for prototype 2*

Validation: Prototype 1 and 2 have been validated through the experimental setup as shown in Figure 4. Responses of these prototypes have been measured by a vector network analyser (VNA) with the model of N5230A PNA-L.

For the validation and coding, amplitude responses of S_{21} parameter has been extracted. Furthermore, the measured response of S_{21} parameter has been compared with its corresponding simulated response as presented in Figure 5 for prototype 1 and Figure 6 for prototype 2. As stated earlier, all resonators are present on prototype 1, the response is in full agreement with the proposed idea that is, each resonator has its corresponding resonance with 9 distinct dips within the spectrum from 4.5 to 6 GHz. Thus, this gives the coding as 111111111 both from the simulated and measured responses as presented in Figure 5. Similarly, from Figure 6, it is seen that there are only six distinct dips in the spectrum. Since three resonators are shorted, their corresponding resonances are absent within the spectrum by leaving the '0' logic states on their frequency positions. Whereby, other six resonators that are not shorted on the prototype 2 represent the logic '1' states and hence generate the coding combination as 110110101.

To validate for the full system, these two prototypes have been connected with Tx and Rx antennas while using the same VNA. Figure 7 shows the measurement setup for the full system validation, where, the VNA with antennas works as the reader, and a prototype with antennas works as the tag. The Tx antenna of the reader is connected at VNA

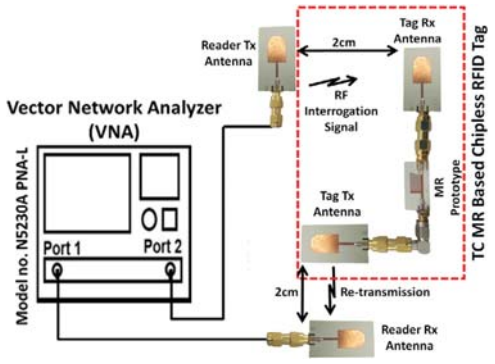

Fig. 7 *Measurement setup for full system validation*

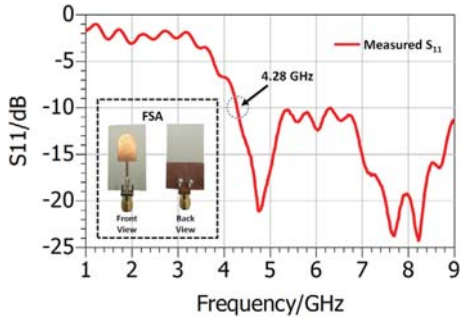

Fig. 8 *Measured S_{11} response of the FSA*

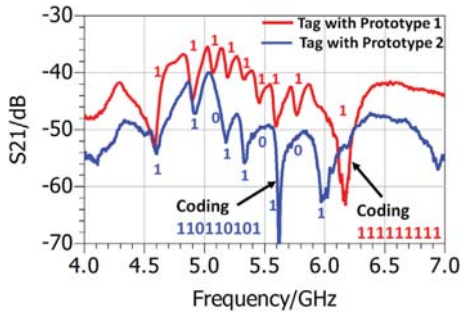

Fig. 9 *Measured S_{21} (amplitude) with tag prototypes and the reader*

port 1 while having the same polarization with the Rx antenna of a tag. Similarly, the Tx antenna of a tag and the Rx antenna of the reader are matched in polarization. A distance of 2 cm has been kept between the reader and a tag due to the low RF power generation by the VNA. The antenna used here is a newly designed planar microstrip fingertip-shaped antenna (FSA) with partial ground plane. The measured S_{11} response of the FSA is shown in Figure 8. Like the TCMR, the same substrate material has been used to design the FSA. The S_{11} response shows that the antenna works from 4.28 GHz and continues working beyond 9 GHz which is required for the system validation. Figure 9 shows responses (S_{21}) of the chipless tag both for prototype 1 and 2 while measured with the entire system. It has been observed that the extracted coding combinations are exactly same as when these prototypes where not in the full system. The tag with prototype 1 gives the coding of 111111111 and the tag with the prototype 2 gives the coding combination of 11011010. A slight shift occurs in the resonant frequencies due to the fabrication issues.

Thus, it is evident that different bit combinations can be generated with the designed TCMR-based tags for retransmission-based chipless RFID applications. Table 1 summarizes the comparison between TCR and other resonators for the occupied area by a single resonator only. From the comparison, it is found that up to 86.7% of the resonator's occupied area can be reduced with the implementation of TCR for retransmission-based chipless RFID system.

Table 1. Comparison between TCR and other resonators

Ref	Resonator ype	Resonator Occupied Area [mm^2]	Recudecd area with TCR
[1]	MRSR	31.2	66.83%
[3]	MRSR	11.4	9.2%
[4]	Rectangular (Tristate)	34	69.6%
[5]	Rectangular (K-state)	51.7	80%
[6]	MCSR	77.85	86.7%
[2]	MCSRR	11.125	7%
[7]	CSRR	36	71.25%
This Work	TCR	10.35	

Conclusion: Two differently coded 9-bit prototypes have been designed and developed with the TCMR and validated through measurements that have good agreements with simulations. Prototypes of chipless tags have been implemented with the two TCMRs connected to the newly designed antennas. The entire system has been validated where the VNA works as the reader. From the S_{21} measurement of a tag, the coding combination has been extracted as 111111111 when all resonators are present and 110110101 when three resonators are absent. One of the remarkable aspects of TCMR is that 9 bits can be imposed by utilizing the width of one MRSR that produces only 1 bit. Furthermore, a maximum reduction of 86.7% in terms of the occupied area of the resonator has been achieved. This work is expected to be further elaborated for item tagging and sensing applications.

Acknowledgments: This work has been partially funded by the Center for Research Innovation and Management (CRIM), Universiti Teknikal Malaysia Malaka (UTeM) and in collaboration with Department of Electrical and Computer Engineering (ECE), Faculty od Engineering, International Islamic University Malaysia (IIUM).

Received: *28 August 2020* Accepted: *1 October 2020*
doi: 10.1049/ell2.12036

References

1 Preradovic, S. et al.: Multiresonator-based chipless RFID System for Low-cost item tracking. *IEEE Trans. Microwave Theory Tech.* **57**(5), 1411–1419 (2009)
2 Bhuiyan, M.S., Karmakar, N.C.: An efficient coplanar retransmission type chipless RFID tag based on dual-band McSrr. *Prog. Electromagn. Res.* **54**, 133–141 (2014)
3 Majidifar, S. et al.: A novel phase coding method in chipless RFID systems. *AEU - Int. J. Electron. Commun.* **69**(7), 974–980 (2015)
4 Abdulkawi, W.M., Sheta, A.A.: High coding capacity chipless radiofrequency identification tags. *Microwave Opt. Technol. Lett.* **62**(2), 592–599 (2020)
5 Abdulkawi, W.M., Sheta, A.-F.A.: K-State resonators for high-coding-capacity chipless RFID Applications. *IEEE Access* **7**, 185868–185878 (2019)
6 Hossain, A.K.M.Z., Motakabber, S.M.A., Ibrahimy, M.I.: Microstrip spiral resonator for the UWB Chipless RFID Tag. In Selvaraj, H., Zydek, D., Chmaj, G. (Eds.): *Progress in Systems Engineering*. Springer International Publishing, Berlin, pp. 355–358 (2015)
7 Ma, Z.-H. et al.: A re-transmitted chipless tag using CSRR coupled structure. *Microsyst. Technol.* **24**(10), 4373–4382 (2018)
8 Vena, A., Perret, E., Tedjini, S.: Chipless RFID tag using hybrid coding technique. *IEEE Trans. Microwave Theory Tech.* **59**(12), 3356–3364 (2011)
9 Ibrahimy, M. I., Hossain, A. K. M. Z., Motakabber, S. M. A.: Linear microstrip resonator for UWB RFID Tag. *Int. J. GEOMATE* **13**(40), (2017)